Self-addressing two-photon cavity solitons

R. Vilaseca, M.C. Torrent, J. García-Ojalvo
Departament de Física i Enginyeria Nuclear, Universitat Politècnica de Catalunya, Colom 11, E-08222 Terrassa, Spain

M. Brambilla
Dipartimento di Fisica and INFM, Politecnico di Bari, Via E. Orabona 4, I-70126 Bari, Italy

M. San Miguel
Instituto Mediterráneo de Estudios Avanzados, Universitat de les Illes Balears, E-07071 Palma de Mallorca, Spain

We show that broad-area cascade lasers support the spontaneous formation of two-dimensional bright localized structures in a dark background. These cavity solitons consist of islands of two-photon emission embedded in a background of single-photon emission. We discuss the mechanisms through which these structures are formed, along with their properties and stability. Self pulsation of single solitons and turbulent motion of multiple interacting solitons are also described.

PACS numbers: 42.65.Sf, 42.50.Hz, 42.65.Tg

Spatial solitons are among the most fascinating nonlinear localized structures exhibited by spatially extended systems. In an optical context, these localized structures take the form of self-trapped light beams that propagate through nonlinear media with an unperturbed transverse cross section, and result from a dynamic balance between a spreading linear mechanism (diffraction) and a nonlinear shrinking one [1]. Spatial solitons might be useful for efficient all-optical parallel signal transmission and processing.

Although spatial solitons were initially associated with conservative systems, investigations in last years have shown that similar structures can also appear in dissipative systems. Presently there is a large interest in investigating the case of a nonlinear optical medium placed within a cavity (or near a mirror), in which the influence of feedback and resonance effects leads to localized structures with distinctive qualitative and quantitative characteristics [2]. These *cavity solitons* (CS) often result from a bistability between two stationary spatially-extended states of the system, in the form of either self-trapped switching waves between two homogeneous states, or isolated pattern elements embedded in an homogeneous background. They have been predicted or observed so far in passive (i.e. externally driven) systems with (i) absorptive and/or dispersive nonlinearities [3,4] (semiconductor microresonators [5], vectorial Kerr resonators [6], and single-mirror feedback setups [7]); (ii) second-order nonlinearities (optical parametric oscillators [8] and second harmonic generation [9]); and (iii) third-order nonlinearities (four-wave mixing [10]). They have also been reported in cavities enclosing photorefractive media [11] and lasers with saturable absorber [12].

In this paper we show that cavity solitons also appear in another class of nonlinear optical system, where the fundamental light-matter interaction processes differ from those considered in any of the cases pointed out above, displaying a number of distinctive properties. In particular, in contrast with those cases, our proposed optical system contains only a purely active medium inside the cavity. While standard single-photon lasers cannot exhibit localized structures in the absence of additional intracavity elements, we show here that *two-photon* lasers exhibit them in a natural and spontaneous way, near a domain of bistability between two-photon and single-photon processes. Some further features, such as the unstable and travelling-wave character of one of the bistability branches, the appearance of a background circular modulation not related to a supercritical Hopf bifurcation, and the combined short/long-range character of the soliton interaction are also discussed below.

We consider a cascade laser, in which two fields of different frequency are simultaneously generated through their coupling with the two consecutive transitions defined by a three-level atomic system (Fig. 1). Interaction between these two fields comes through the population of the intermediate level 0 and the two-photon quantum coherence between levels 1 and 2. Transverse effects have been seen to lead in this system to coupled patterns of the two generated fields, in both low-Fresnel-number [13] and high-Fresnel-number (broad-area) [14] cavities. In what follows we will concentrate on the latter case. The spatiotemporal behavior of a cascade laser in such a situation can be described by the following Maxwell-Bloch equations [14]:

$$
\begin{aligned}
\dot{\alpha}_1 &= -\sigma_1\alpha_1 + i\sigma_1\rho_{01} + ia_1\nabla^2\alpha_1 \\
\dot{\alpha}_2 &= -\sigma_2\alpha_2 + i\sigma_2\rho_{20} + ia_2\nabla^2\alpha_2 \\
\dot{\rho}_{01} &= -(1+i\delta_1)\rho_{01} - i\alpha_1 d_1 + i\sqrt{\chi}\alpha_2^*\rho_{21} + \beta_1\xi_1 \\
\dot{\rho}_{20} &= -(1+i\delta_2)\rho_{20} - i\alpha_2 d_2 - i\alpha_1^*\rho_{21}/\sqrt{\chi} + \beta_2\xi_2 \\
\dot{\rho}_{21} &= -(\Gamma+i\epsilon)\rho_{21} - i\sqrt{\chi}\alpha_1\rho_{20} + i\alpha_2\rho_{01}/\sqrt{\chi} \\
\dot{d}_1 &= -bd_1 - 2\,\mathrm{Im}(\alpha_1\rho_{01}^*) + \chi\,\mathrm{Im}(\alpha_2\rho_{20}^*) \\
\dot{d}_2 &= b(r_2-d_2) + \chi^{-1}\,\mathrm{Im}(\alpha_1\rho_{01}^*) - 2\,\mathrm{Im}(\alpha_2\rho_{20}^*)\,,
\end{aligned}
\qquad (1)
$$

where α_1 and α_2 are the complex envelopes of the generated electric fields, ρ_{ij} the complex one- and two-photon coherences, d_1 and d_2 the population inversions of the two transitions, r_2 the pumping rate for the upper level 2, a_1 and a_2 the diffraction coefficients, σ_i, Γ and b the relaxation rates, and χ the efficiency of transition 1 versus transition 2. The cavity detunings for the two fields are given by $\delta_i \equiv \omega_{\rm tr,i} - \omega_{\rm cav,i}$ (with $\omega_{\rm tr,i}$ denoting the transition frequency and $\omega_{\rm cav,i}$ the cavity resonance frequency), and $\epsilon = \delta_1 + \delta_2$. Spontaneous emission processes are accounted for by gaussian white noise terms $\xi_i(\vec{x}, t)$ with zero mean and intensity β_i^2.

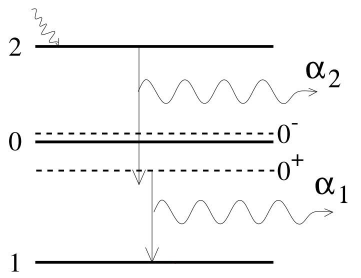

FIG. 1. Energy-level scheme of a cascade laser in two-photon resonance. Arrows indicate the cavity frequencies.

Since pumping is assumed to act only on the upper transition, laser emission occurs first, for increasing pumping rate, only in field α_2. If the cavity detuning for this field is negative ($\delta_2 < 0$), which is the situation that we will assume in what follows, then it is well known [15] that the transverse profile of the field is homogeneous and its frequency ω_L is given by the pulling formula $\delta_L = \delta_2/(\sigma_2 + 1)$, where $\delta_L = \omega_{\rm tr,2} - \omega_L$. Field α_2 induces an ac-Stark splitting of level 0 (Fig. 1), so that field α_1, when generated, has two possible resonance frequencies (Autler-Townes doublet) occurring at cavity detunings given by $\delta_1^{\pm} = \frac{1}{2}\left(\delta_L \pm \sqrt{\delta_L^2 + 4\alpha_2^2}\right)$. These values correspond to resonance with levels 0^+ and 0^-, and are associated, for large $|\delta_2|$, to two-photon and step-by-step (i.e. single-photon) processes, respectively [16].

Let us focus on the case of two-photon resonance, $\delta_1 = \delta_1^+$. In the absence of transverse effects [$a_1 = a_2 = 0$ in Eqs. (1), homogeneous-field approximation], Fig. 2 shows (in continuous and dashed lines) the steady-state intensities versus the pump parameter r_2, for $|\delta_2|$ large ($\delta_2 = -20$) and $\delta_1 = \delta_1^+$. By increasing r_2, the zero-intensity solution first undergoes a supercritical pitchfork bifurcation (PB) at $r_2 = r_2^{\rm PB}$, leading to emission of field α_2, followed by a subcritical PB at $r_2 = r_2^{\rm th}$, which leads to emission of α_1 as well. Due to this second bifurcation, the system abruptly jumps to a two-photon branch with large intensity for both fields α_1 and α_2, because of the weak initial saturation of two-photon processes [17]. As shown in Fig. 2, two domains of bistability appear: one for $r_2^{\rm SN} < r_2 \leq r_2^{\rm PB}$, involving the two-photon (upper) branch and the zero-intensity solution, and another for $r_2^{\rm PB} < r_2 \leq r_2^{\rm th}$, involving the two-photon branch and the single-field branch. As will be shown below, the second of these domains will be at the origin of CS formation.

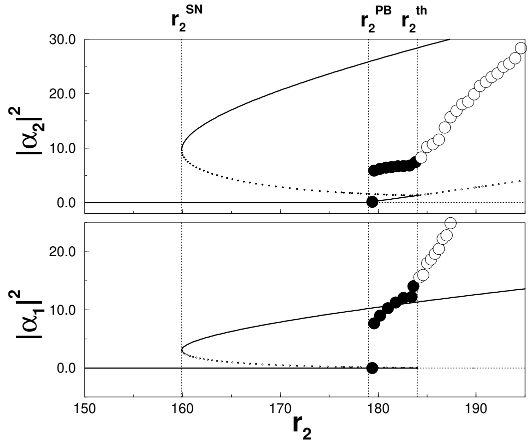

FIG. 2. Field intensity vs. pumping for a cascade laser, for $\delta_2 = -20$ and $\delta_1 = \delta_1^+ = 13.33$. Solid (dashed) lines: stable (unstable) steady solutions in the homogeneous-field limit. Full circles: soliton peak intensity; empty circles: time-averaged maximum peak intensity ($\sigma_1 = \sigma_2 = 0.5$, $b = \Gamma = 1$, and $\chi = 0.76$).

When transverse effects are taken into account, important changes take place. First, both resonances of the field α_1 with the atomic levels 0^- (step-by-step processes) and 0^+ (two-photon processes) can occur simultaneously, for the same value of the cavity detuning δ_1 [16]. This is shown in Fig. 3(a), which represents the neutral stability curve (obtained from a linear stability analysis of the single-field emission regime $\alpha_1 = 0$, $\alpha_2 \neq 0$) for the same parameter values of Fig. 2. In Fig. 3(a), k represents the wavenumber of a perturbation in the form of a transverse traveling wave affecting the field α_1. Above the neutral stability curve, the perturbation grows. Minima occur at two values of $|k|$, given by $|k| = 0$ and $|k| = \sqrt{\delta_1^+/a_1}$. The first value means generation of a homogeneous field α_1 due to resonance with level 0^+ (two-photon emission). In contrast, the second value corresponds to the generation of a transverse traveling wave for α_1, which allows this field to be in resonance with level 0^- (step-by-step emission). As it also occurs in simple two-level lasers with positive detuning [15], generation of the transverse component leads to emission of a tilted wave with an increased wavenumber and frequency.

As shown in Fig. 3(a), the threshold is exactly the same for the two minima (dashed line), and coincides with that found above in the case of the homogeneous-field approximation ($r_2^{\rm th}$). Just below this threshold, the spontaneous (noise-induced) emission on field α_1 occurs predominantly through single-photon, step-by-step processes (i.e., with $|k| = \sqrt{\delta_1^+/a_1}$). However, when pumping is increased above $r_2^{\rm th}$, two-photon processes take over the nonlinear competition between the two wavenumbers [see Fig. 3(b)]. The faster growth of the two-photon processes can be traced back to their small initial saturation. The result is that, after a short transient, emission occurs in the form of *cavity solitons*, as shown in Fig. 4. This figure portrays typical intensity and phase profiles of the two fields. A first remarkable feature of the CS shown in Fig. 4 is the fact of being the *only* stable emission state of the system. We have checked that the homogeneous-field solution described in Fig. 2 (upper branch), as well as any other close solution in the form of transverse traveling waves (which appear above threshold), are unstable.

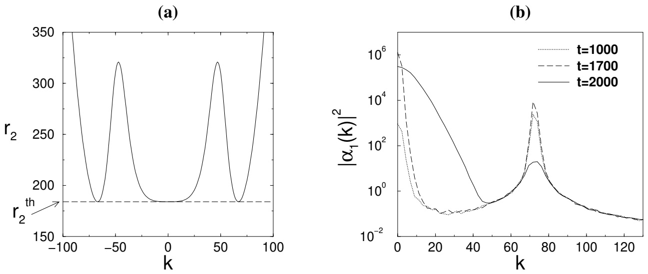

FIG. 3. (a) Neutral stability curve (field-1 emission threshold), for $\delta_2 = -20.0$ and $\delta_1 = 13.33$. (b) Spherically averaged far-field intensity profile of α_1 for $r_2 = 184$, at three different instants of time. Other parameters are those of Fig. 2, plus $a_1 = a_2 = 0.003$.

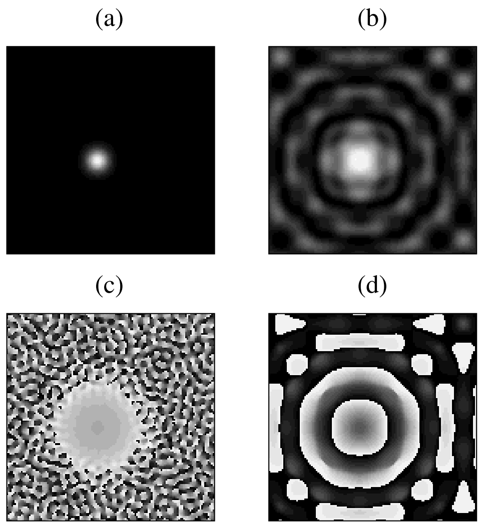

FIG. 4. Transverse emission of a broad-area cascade laser for the parameters of Fig. 3(a), plus $r_2 = 185$ and $\beta_1 = \beta_2 = 10^{-5}$: intensity (a,b) and phase (c,d) profiles of fields α_1 (a,c) and α_2 (b,d). In all plots, maxima is represented by white, and minima by black. In the phase plots, the scale ranges from $-\pi$ to $+\pi$.

The radial cross section displayed in Fig. 5(a) shows that, for field α_1, the CS has a similar form as that of bright solitons appearing in conservative media ($\approx$ *sech*), with a background intensity at the noise level. In contrast, for field α_2 the soliton is surrounded by outward-traveling concentric rings of noticeable amplitude [Fig. 5(b)]. This slowly-decaying circular modulation provides a mechanism of long-range interaction between neighboring α_1-solitons, which arises in spite of their highly localized character.

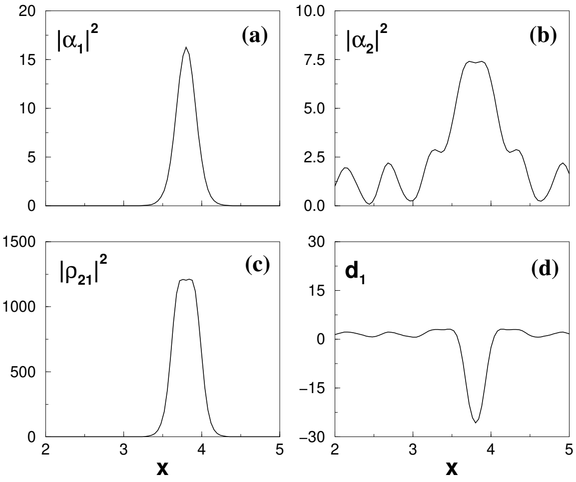

FIG. 5. Radial 1-d section of a 2-d cavity soliton, for the parameters of Fig. 3(a), plus $r_2 = 184$ and $\beta_1 = \beta_2 = 10^{-6}$.

From a physical point of view, the two-photon coherence profile [Fig. 5(c)] reveals that the CS corresponds to an island of *two-photon* emission embedded in a background of *single-photon* (step-by-step) emission. Because of that, the soliton exhibits no population inversion between levels 0 and 1 [Fig. 5(d)], whereas the noisy background of field α_1 has the dominant transverse wavenumber corresponding to the outer minimum of Fig. 3(a), $|k| = \sqrt{\delta_1^+/a_1}$. These facts indicate that CS formation is related in this system to the second of the two bistability regions found in the homogeneous-field approximation ($r_2^{\mathrm{PB}} < r_2 \leq r_2^{\mathrm{th}}$, Fig. 2). This relation is, however, of a different nature from the one present in other systems. In particular, as mentioned above, the upper branch is here unstable. Note also that the peak of α_2 [Fig. 5(b), and black circles in Fig. 2] is much smaller than the corresponding homogeneous value of the upper branch. This is due to the fact that the energy in field α_2 is distributed between the localized spot and the surrounding concentric traveling rings that deeply modulate the background [Figs. 4(b) and (d)]. In addition, we have not found any supercritical Hopf bifurcation (HB) in the lower branch which could be responsible for those rings. This contrasts with the modulation found in [18].

The stability of the CS as a function of the pump parameter is shown as symbols in the bifurcation diagram of Fig. 2. For $178 \lesssim r_2 \lesssim 184$ the CS density is low, and the solitons are stable, with a peak intensity that increases smoothly with r_2 (black circles in the figure). At $r_2 \lesssim 178$, the CS disappears and emission switches off. For $r_2 \gtrsim 184$, neighboring CSs interact with each other through the outer rings of field α_2, as explained above. This interaction usually leads to complex dynamics, eventually producing turbulent motion and birth/death of solitons. Empty circles in Fig. 2 correspond to this regime, and represent the time-averaged maximum intensity of the field. A snapshot of this situation is shown in Fig. 6, where it can be seen that each soliton has its own phase, not shared with other CSs due to the absence of a coupling background. This contrasts with CSs found in externally driven cavities [5]. Beyond $r_2 \gtrsim 190$, CSs start to lose their circular shape and to cover a wider area. Eventually, for $r_2 \gtrsim 200$, most of the transverse plane becomes illuminated, but small dark areas remain which take the form of optical vortices. A similar evolution from CS-dominated to vortex-dominated dynamics has been described in [19]. With respect to the stability of the CSs when changing the detuning parameter we have found that, with increasing $|\delta_2|$ the CS persists up to very large values (up to $\delta_2 \sim -50$, at least), whenever δ_1 remains close to δ_1^+. On the other hand, as a function of δ_1 the CSs exist, in the situation described above ($\delta_2 = -20$), for $13.2 \lesssim \delta_1 \lesssim 15.3$. At $\delta_1 \approx 15.3$ there is a sudden jump to a unique, spatially extended solution in the form of an intensity-uniform traveling wave with a different wavenumber for each field, in which two-photon processes are dominant [20]. For $\delta_1 \lesssim 13.2$, field α_1 is off.

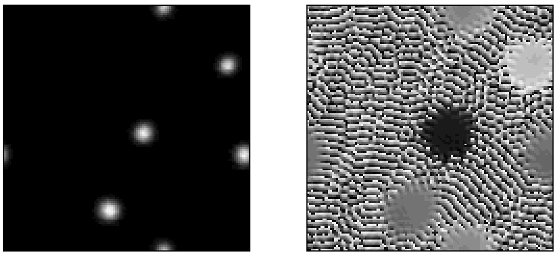

FIG. 6. Interacting cavity solitons: intensity (left) and phase (right) profiles of α_1 for the parameters of Fig. 3(a), plus $r_2 = 190$ and $\beta_1 = \beta_2 = 10^{-6}$.

In conclusion, we have shown that cavity solitons can appear spontaneously in purely active optical media, as a result of the interplay between two-photon and single-photon processes. They show some singular features that have not (or have only partially) been met in other optical systems investigated so far. The recent experimental realization of two-photon amplification [21] sheds hope on the observability of this phenomenology.

We acknowledge financial support from the DGESIC (Spain – projects PB96-0241 and PB98-0935) and Generalitat de Catalunya (project 1999SGR00147).

[1] G.I. Stegeman and M. Segev, Science **286**, 1518 (1999).
[2] L.A. Lugiato, M. Brambilla and A. Gatti, Adv. in At., Mol. and Opt. Phys. **40**, 229 (1999); W. Firth and G. Harkness, Asian J. Phys. **7**, 665 (1998).
[3] N.N. Rosanov and G.V. Khodova, J. Opt. Soc. Am. B **7**, 1065 (1990); M. Tlidi, P. Mandel, and R. Lefever, Phys. Rev. Lett. **73**, 640 (1994);
[4] M. Kreuzer, H. Gottschling, T. Tschudi, and R. Neubecker, Mol. Cryst. Liq. Cryst. **207**, 219 (1991); W.J. Firth and A.J. Scroggie, Phys. Rev. Lett. **76**, 1623 (1996); M. Brambilla, L.A. Lugiato, and M. Stefani, Europhys. Lett. **34**, 109 (1996).
[5] M. Brambilla, L.A. Lugiato, F. Prati, L. Spinelli, and W.J. Firth, Phys. Rev. Lett. **79**, 2042 (1997); D. Michaelis, U. Peschel, and F. Lederer, Phys. Rev. A **56**, R3366 (1997).
[6] R. Gallego, M. San Miguel, and R. Toral, Phys. Rev. E **61**, 2241 (2000); V.J. Sánchez-Morcillo, I. Pérez-Arjona, F. Silva, G.J. de Valcárcel, and E. Roldán, Opt. Lett. **25**, 957 (2000).
[7] A. Schreiber, B. Thuring, M. Kreuzer, and T. Tschudi, Opt. Commun. **136**, 415 (1997); B. Schäpers, M. Feldmann, T. Ackemann, and W. Lange, Phys. Rev. Lett. **85**, 748 (2000).
[8] V.J. Sánchez-Morcillo, E. Roldán, G.J. de Valcárcel, and K. Staliunas, Phys. Rev. A **56**, 3237 (1997); S. Longhi, Phys. Scripta **56**, 611 (1997); G.L. Oppo, A.J. Scroggie, and W.J. Firth, J. Opt. B **1**, 133 (1999); M. Le Berre, D. Leduc, E. Ressayre, and A. Tallet, J. Opt. B **1**, 153 (1999).
[9] C. Etrich, U. Peschel, and F. Lederer, Phys. Rev. Lett. **79**, 2454 (1997).
[10] V.B. Taranenko, K. Staliunas, and C.O. Weiss, Phys. Rev. Lett. **81**, 2236 (1998).
[11] M. Saffman, D. Montgomery, and D.Z. Anderson, Opt. Lett. **19**, 518 (1994).
[12] V.Y. Bazhenov, V.B. Taranenko, and M.V. Vasnetsov, Proc. SPIE **1840**, 183 (1992); N.N. Rosanov, S.V. Fedorov, and G.V. Khodova, Physica D **96**, 272 (1996); V.B. Taranenko, K. Staliunas, and C.O. Weiss, Phys. Rev. A **56**, 1582 (1997).
[13] J. García-Ojalvo, M.C. Torrent, R. Vilaseca, and M. Brambilla, Chaos, Solitons & Fractals **10**, 819 (1999).
[14] J. García-Ojalvo, R. Vilaseca, and M.C. Torrent, Phys. Rev. A **56**, 5111 (1997).
[15] P.K. Jakobsen, J.V. Moloney, A.C. Newell, and R. Indik, Phys. Rev. A **45**, 8129 (1992).
[16] J. García-Ojalvo, R. Vilaseca, and M.C. Torrent, Europhys. Lett. **43**, 261 (1998).
[17] E. Roldán, G.J. de Valcárcel, R. Vilaseca, and V. Espinosa, J. Mod. Opt. **44**, 83 (1997).
[18] M. Tlidi and P. Mandel, Phys. Rev. A **59**, 2575 (1999).
[19] C.O. Weiss, M. Vaupel, K. Staliunas, G. Slekys, and V.B. Taranenko, Appl. Phys. B **68**, 151 (1999).
[20] M.C. Torrent, R. Vilaseca, and J. García-Ojalvo, J. Opt. B **2**, 432 (2000).
[21] O. Pfister, W.J. Brown, M.D. Stenner, and D.J. Gauthier, Phys. Rev. A **60**, R4249 (1999).